Front. Optoelectron. 2014, 7(4): 425–436
DOI 10.1007/s12200-014-0416-4

RESEARCH ARTICLE

Optical design in high density and high capacity multi-layer data storage system

Yuzuru TAKASHIMA (✉)

College of Optical Sciences, University of Arizona, Tucson, AZ 85721, USA

Abstract Fundamental requirements for optical system design for volume recording system is identified. Anastigmatic objective lens design is required for conventional page-based system, whereas for multi-layer volume recording systems, an Aplanatic and zoom optical design is needed with an afocal sub-optical system including a high numerical aperture (NA) objective element. An NA 0.4 and four element design is feasible by only using off-the-shelf components. Recording depth ranges of 0.4 mm for wavelength 532 nm and 0.2 mm for 405 nm. The design demonstrates sufficiently small as-built wavefront error, less than 0.1 waves while implementing focusing and tracking capabilities to the design.

Keywords holographic and volume memories, lens system design, optical disks

1 Introduction

Optical data transmission is widely adopted for long haul data transfer due to its high speed and non interfering nature. Such an infrastructure enables high speed content distributions such as HD movies, e-books and extensive music libraries. In addition, the Internet of Things (IoT) which connects things such as consumer appliances over the Internet is of interest [1]. Consequently, bandwidth demand on user side has been increased accordingly to handle personal data. For enterprise and professional use, handling of data, especially the power consumption required to store the data became a serious bottleneck to keep up with the explosion of data.

Although hard disc drives are mainly used in data centers, optical data storage is considered as a viable option. Especially, far-field optical recording has unique capability such as very low storage cost per bit for the lifetime of the data, and long-term stability of data, thanks to the fact that the power consumption is nearly zero for the most of the period of archiving. Thus, high density optical data storage in the far field recording scheme is an attractive add-on to the existing hard disc based data center to add archiving capabilities.

To achieve high density of over 1 TByte, a volumetric recording has been actively investigated in far-field regime. Such volumetric recordings are categorized into two major schemes, volume holographic recording and multi-layer volumetric recording. In the far-field recording scheme, the numerical aperture (NA) of optics and wavelength are two critical factors to determine recording density. Besides, it is proposed incorporating superposition of two orthogonal polarizations and information absorption spectrum to increase recording density. With almost all the techniques to enhance recording density, volumetric recordings are compatible. Thus it is the most effective way toward far-field based high density recording system. However, it is still an open question which volumetric recording is the best option to be pursued. Some theoretical analysis revealed fundamental similarity and difference of performance for specific pair of recording schemes. For example, McLeod et al. reported the performance of the page-based volumetric and bit-based multi-layer holographic systems are comparable in data rate, data capacity are comparable [2]. Based on the analysis, Takashima and Hesselink reported that under the presence of perturbations, the performances of two system differently varies as a function of NA of optic when the 3rd order aberrations are taken into account [3]. The 1st and 3rd order analysis indicates in optical design, difference in the recording scheme has to be appropriately taken into account in the practice of optical system design.

In this paper, we report optical design method for volume recordings while emphasizing the procedure to determine specification for optical designs based on fundamental first order optics and 3rd order aberration

Received January 31, 2014; accepted July 24, 2014

E-mail: ytakashima@optics.arizona.edu

theory. It is also of our interest to see how the 1st and 3rd order requirement can be implemented as a train of lens elements to satisfy the specifications.

In this research paper, first, we review the design of an objective lens for volumetric holographic recording. Second, it is followed by discussing in detail on 1st order design principles for the multi-layer bit based recording, since optical designs for multi-layer recording are not fully investigated. We also present a viable optical design for a multi-layer recording demonstration platform by only using only and with minimum number of off-the-shelf components.

The design approach would give a partial answer for the question, which recording scheme works better from the view point of optical system design. The all off-the-shelf design can be used as a benchmark in multi-layer volume recording, from which optical performances are further improved.

2 Optical design method for volumetric recording

2.1 Optical design for volume holographic recording

Optical designs of objective lenses for the volume holographic recording have been reported by several authors [4–6]. There exists a clear difference in lens designs between volumetric holographic recording and multi-layer recording. Multi-layer recording is extension of surface recording to depth dimensions. The surface recording system requires an Aplanatic objective lens for which spherical aberration and Coma are compensated [7,8]. This is because the objective lens is not solely operating on-axis condition, but rather in an off-axis condition due to an imperfect assembly of the objective lens to optical system. Also, the lens focuses a laser beam under the presence of mechanical perturbations such as tilt induced by rotation of recording media. The tilt of the media induces substrate induced Coma. Therefore, controlling of media tilt is crucial for assuring the off-axis performance of the objective lens.

For the volumetric holographic recording, data capacity is increased by superimposing multiple holograms using Bragg selectivity. Consequently, requirements for optical design are mainly imposed by the Bragg selectivity. Figure 1(a) shows a schematic of the volumetric holographic recording system. Since the archiving is the primary purpose of far-field recording, we consider removable media system, i.e., recording and retrieval is employed at different disc drive platforms. For example, once information is recorded at platform 1, recording media is removed and retrieved later at the platform 2. At platform 1, a spatial light modulator (SLM) is placed at the front focal point of the lens 1 (L1) and is coherently illuminated. The image bearing beam at the back focal plane of the lens L1 interferes with a reference beam (R), and forms a Fourier transform hologram. We assume that holograms are multiplexed by employing angular multiplexing by changing the angle of incidence of R with respect to recording media [9]. Upon retrieval of the data, the recording medium is transferred to the platform 2, and is illuminated by reconstructions reference beam (R′) while varying the angle of incidence with respect to the media. The reconstructed Fourier hologram is inversely Fourier transformed by the second lens (L2), and is detected by a two-dimensional sensor array such as a charge coupled device (CCD). From the viewpoint of geometrical optics, the interchangeable media system is equivalent to a time delayed imaging system with forward and inverse Fourier transforms. By examining Fig. 1(b), we notice that there are two kinds of imaging are involved, the object imaging and pupil imaging. For the object imaging, the SLM and CCD are conjugates, i.e., object and image. Whereas for the pupil imaging, an object located at negative infinity with respect to L1 is imaged at the location of positive infinity with respect to the second lens L2. In other words, the pupil imaging is focusing of the collimated beam on the recording medium followed by re-collimation of the focused light by the second lens L2. For volume holographic imaging, the pupil imaging is especially important in two aspects, 1) mapping of SLM images to CCD and 2) performing exact Fourier transform [10]. The accuracy of the mapping is crucial, especially for volume holographic recording system without employing quasi phase conjugate readout [11]. Although for holographic recording as far as the mapping of SLM pixel image to the CCD is well defined, there is no physical significant requirement on the mapping. Also, exact Fourier transform of the SLM image is not necessary either. However, assuring the media transfer capability among platforms requires well-defined mapping. Consequently, the mapping of $h = f \sin\theta$, where h is the marginal ray height for pupil imaging, and is also height of the chief-ray for objet imaging, θ is the angle of the ray at Fourier plane, and f is the focal length of the lens, the most appropriate mapping if we consider the relations of objects and pupil aberrations [12,13].

Table 1 summarizes relations between object and pupil aberrations. For the object imaging, there are at least three primary Seidel aberrations, such as spherical aberration, Coma, and astigmatism to be corrected. Next, we consider pupil Seidel aberrations. Correction of the spherical aberration and Coma is needed to satisfy the Abbe's Sine condition, $h = f \sin\theta$, where h is marginal ray height, f is focal length and θ is marginal ray angle. The relation is known as the Sign condition for an object located at infinity which is the case for pupil imaging.

Aberration theory indicates pupil Coma is automatically corrected for once pupil spherical aberration and the first four object aberrations are corrected in a 4f telecentric system. Thus, corrections of five Seidel aberrations among

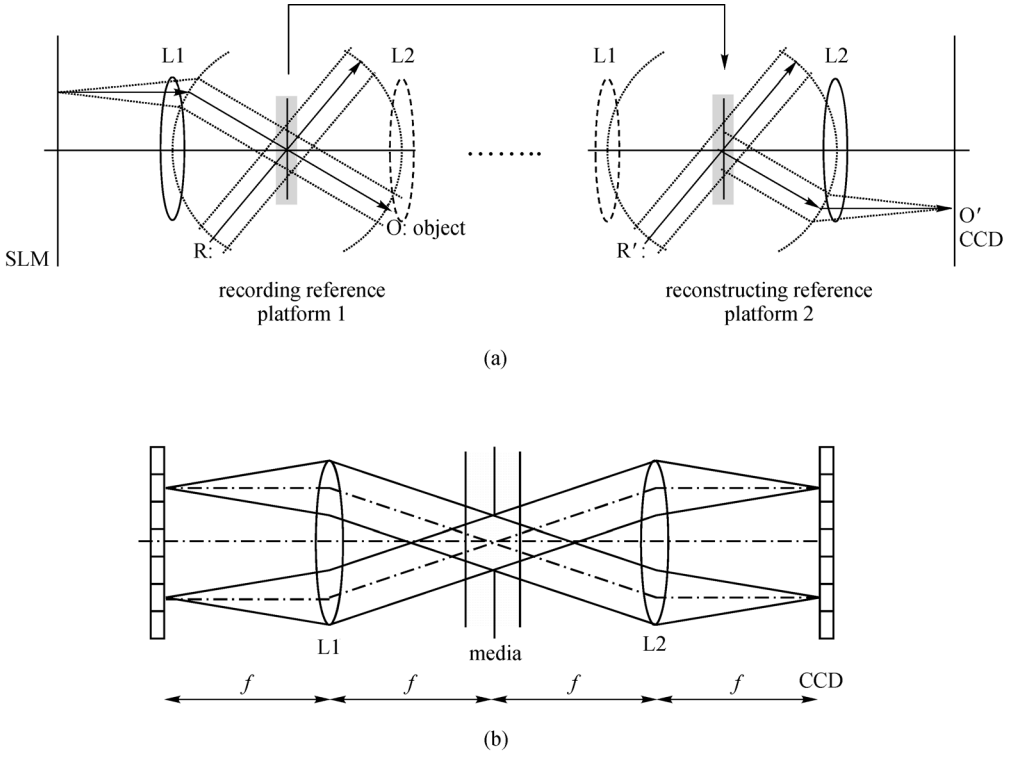

Fig. 1 (a) Schematic of volume holographic recording with interchangeable media; (b) in the lens system, two kinds of imaging are involved, the object imaging (solid line) and the pupil imaging (dashed line). SLM: spatial light modulator; CCD: charge coupled device

Table 1 Relations between object and pupil aberrations

lens aberrations	object imaging	pupil imaging
spherical aberration	corrected	corrected
Coma	corrected	(no Coma if 5 aberrations are corrected.)
astigmatism	corrected	NA
Petzval	corrected	←
distortion	NA (symmetry)	NA (small field of view)

total of ten pupil and object aberrations (three objects, one pupil and one common Petzval) lead to satisfy the design requirements for volumetric holographic recording. Consequently, once we correct the five aberrations listed in Table 1, ray to angle mapping is uniquely determined while satisfying aberration correction for the object imaging. In addition, the mapping relation assures an exact Fourier transform too which is beneficial since well-defined deconvolution kernel for signal processing is usable.

The analysis indicates an Anastigmatic lens is needed for which the first three Seidel object aberrations are corrected. Additional correction of pupil spherical aberration enables using an interchangeable medium. Degree of freedom analysis indicates, aspherical doublet has an enough degree of freedom to satisfy with the aberration correction if varying the power arrangement is included in the degree of freedom. Figure 2 shows design examples obtained by the following traditional lens design procedure [6]. The important conclusion is that the negative power surface close to the Fourier transform plane minimizes aberrations, and consequently increases the NA for object and pupil imaging.

2.2 Optical design for multilayer recording system

The second implementation of high capacity data storage system is a multi-layer volume recording with aplanatic objective. In addition to the aplanatic requirement, correction of a substrate induced spherical aberration is required. Demonstration platforms as well as 3rd order and ray-trace based optical designs for multi-layer recording systems have been reported in literatures [2,14,15].

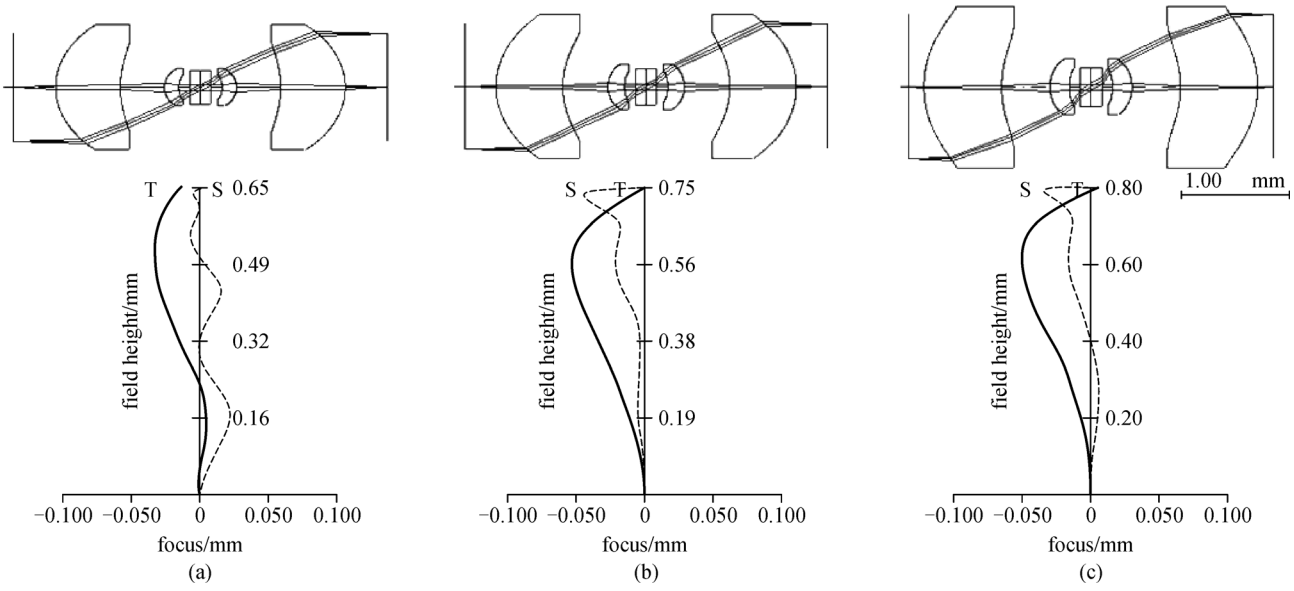

Fig. 2 Design example of Anastigmatic lens for volume holographic recording using for (a) NA = 0.7 (N = 1.59219); (b) NA = 0.75 (N = 1.85078) and (c) NA = 0.8 (N = 2.15858). A strong negative surface close to the Fourier plane improves object imaging 2.2. Saggital (S) and tangential (T) field aberration are plotted for each of the design

However, fundamental requirements and constraints on 1st order optical design have not yet been fully addressed. In this section, we address the 1st order design and complete optical design for multi-layer and micro holographic data storage demonstration platform by using only off-the-shelf optical components.

In the first order, lens power arrangements for objective lenses having a capability to access to multiple recording layers are needed. The typical way to implement such optics is described as follows. First, a virtual or real intermediate image is formed by a movable optic or "zooming" optics. Then, the intermediate image is relayed to a final focal point inside a recording medium by a secondary optics including high NA objective elements next to the recording medium. Moving the first optics along optical axis alters conjugate ratio between the intermediate image and final image, therefore, the final image position also moves, which ends up with selection of recording layers. The approach is a rather simple one. However, we immediately notice several drawbacks of the approach. First, the system focal length varies as a function of the writing depth which may require additional components such as a variable aperture to keep the numerical aperture constant. In addition, tuning of the laser power to keep NA and read/write power constant might be additionally needed. Second, the location of the final image nonlinearly moves with respect to the movement of the zooming element. This would impose an additional requirement on actuators for selection of writing depth which typically has a constant spacing between adjacent recording layers.

Ideally, the objective lens for multi-layer recording system has to have an optical power arrangement with constant focal length. Also it is ideal to have a constant NA over the range of multi-layer as well as linear movement of zooming element. Figure 3 shows a schematic diagram of the objective element. The objective element is placed close to the substrate of the recording layer with a constant working distance (WD). Upon moving an optical components (zooming elements), the WD can be kept invariant while back focal length (b_f) varies to access to multiple recording layers throughout the volume of the recording material. Moreover, ideally system focal length (f_{sys}) needs to be invariant to the location of the zooming element to keep the NA constant and the b_f linearly moves with f_{sys}.

Figure 4 shows a conventional power arrangement of variable focus depth objectives for multi-layer optical data storage. For simplicity, we have depicted that both of the zooming and relay optics are positive thin lenses. For the relay optics (Fig. 5), within first-order optics, $\theta' = \theta(t^*\phi - 1)$ holds for the zooming optics, where t is the location of the intermediate image measured from relay optics, ϕ is a power (inverse of the focal length) of the relay optics, θ and θ' are angles of marginal rays at the side of intermediate image and the final image, respectively.

Making a focal length invariant for all the zooming range is equivalent to having an invariant emerging ray angle (θ') at the side of the final image. As a result, a condition $\theta\ (t^*\phi - 1)$ = constant, is needed. Apparently, a single zooming optics cannot satisfy the requirement since θ is a constant while t is a variable. We consider next minimum option for zooming optics consisting of two elements. Figure 5 shows a schematic of power arrangement. We limit analysis for the case of using two positive

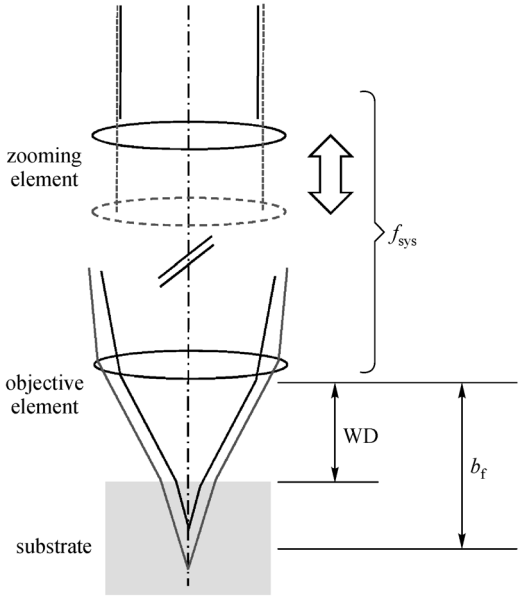

Fig. 3 Schematic of 1st order power arrangement of objective zoom lens for multi-layer recording. WD: working distance

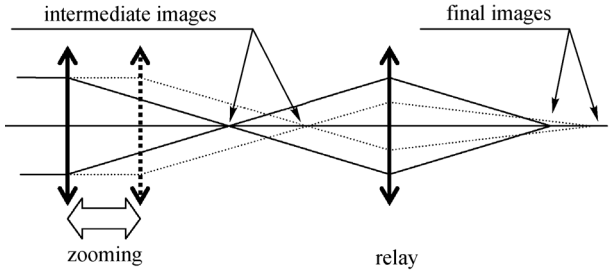

Fig. 4 Power arrangement of conventional variable focus depth objectives

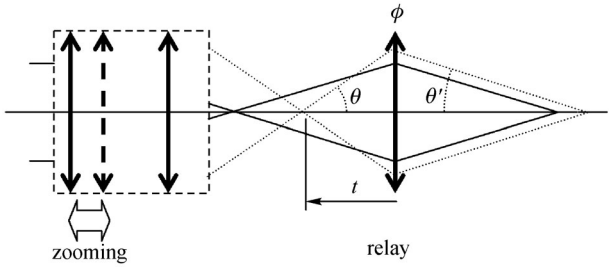

Fig. 5 Powerful arrangement of variable focus depth objectives with a constant focal length

or two negative elements. We also have two possible selections on zooming element between two. Among a total of four possible power arrangements, only positive-positive combination with moving first element satisfies the condition aforementioned. In Fig. 6, power arrangement of the three element zoom objective design is depicted.

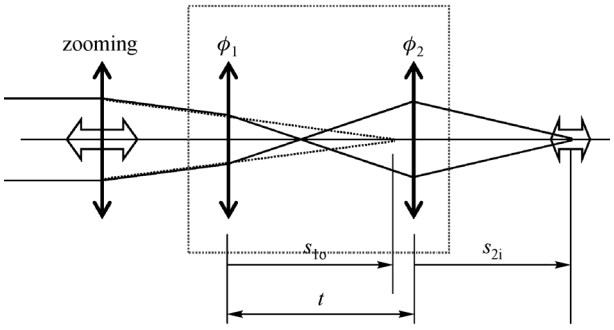

Fig. 6 Power arrangement of the three elements zoom objective design

The first element, zooming element and the second element with optical power ϕ_1 form an intermediate image between the 2nd lens and the 3rd lens. The location of the intermediate object measured from the 2nd element is s_{1o}. The distance between the 2nd and the 3rd element is t. The location of the final image is at the distance of s_{2i} from the 3rd element. We consider the focal length of the subsystem, the 2nd and the 3rd elements $f_{sys} = \phi_1+\phi_2-t\,\phi_1\phi_2$. The first order analysis indicates

$$\frac{ds_{2i}}{ds_{1o}} = (1-\phi_2 t + s_{1o} f_{sys})^{-1}. \quad (1)$$

Apparently, under the condition of $f_{sys} = 0$, ds_{2i}/ds_{1o} is a constant. Therefore, the linearity of the shift of the image location to shit of the zooming element is satisfied. This means the 2nd and the 3rd lenses are an afocal system as a combined lens system. The afocal characteristics automatically satisfies requirement of constant NA over the shift of zooming element.

Figure 7 shows the power arrangement of the three elements zoom objective with afocal design. The afocal system has a constant angular magnification θ_{out}/θ_{in} = constant, where θ_{out} and θ_{in} are angles of incidence of marginal ray at the right hand side and left hand side space, respectively. The angle θ_{in} does not change with the movement. This means that θ_{out} does not change either. As a result, $\sin\theta_{out}$, NA/n, where n is index of refraction of the substrate material, is a constant over the zooming. Note that, even being able to implement such additional features, the proposed optical power arrangement requires only one moving component. Thus, our approach inherits the simple implementation of the conventional approach. Importantly, such a minimum optical power arrangement is possible only if a specific combination of power is adopted for the zooming optical component.

Figure 8 summarizes the power arrangement. The point Pi is formed by a Focusing element, which moves along the optical axis. The intermediate image at Pi is re-imaged by relay lens assembly consisting of aberration compensator (AC) and aspheric objective element (OE). The focus point compensator (FPC) is placed near the intermediate

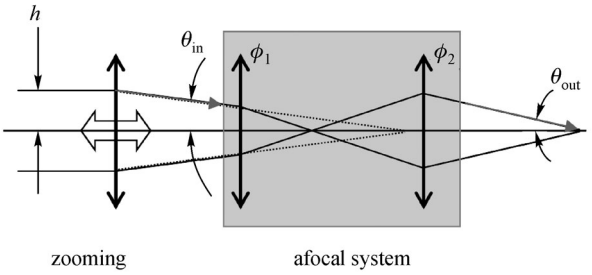

Fig. 7 Power arrangement of the three elements zoom objective with afocal design

image Pi. The FPC compensates variation of the system focal length induced by zooming of FE. All the components are placed to satisfy the 1st order power arrangement, and the final image is formed at the location indicated as Pf.

Moving the FE changes the conjugate ratio between Pi and Pf , this changes ray incident height of the relay lens assembly. The change of ray incident height on the OE as well as the change of the conjugate ratio induces aberration, because the OE is designed for a specific ray height and conjugate ratio to minimize aberrations. To compensate the induced aberration, aberration correction element (ACE) is added. The ACE re-collimates rays from the intermediate point Pi. As a result, the variation of marginal ray height as well as changes in the conjugate ratio for the OE itself is reduced. The arrangement enables using the OE designed for specific conjugate ratio in the proposed zoom design.

3 Optical design of demonstration platforms for multi-layer micro holographic data storage

Two kinds of demonstration platforms adopt the first order design by only using commercially available off-the-shelf optics. The first design example employs a 532 nm diode pumped solid state (DPSS) laser operating at 532 nm. The system is designed to write and read single bit micro holograms. The second design example employs blue laser diode with 405 nm. The 405 nm system is designed to read and write multiple bits simultaneously to further increase data transfer rate. Figure 9 shows a schematic diagram of multi-layer micro holographic data storage. Unlike to multi-layer recording systems using phase change material, micro holographic data storage requires two counter propagating and tightly focused laser beams, object and reference beams need precise overlapping on top of each other. Thus, servo mechanism is needed to keep overlapping of the beams for writing and to precisely align reconstructing beam to the hologram for the readout. Consequently, the zoom objective design has to be compatible with the servo system. The second platform employs three 405 nm blue lasers so that three micro holograms can be read out simultaneously. In this section, optical architecture of the demonstration platform is discussed, and it is followed by a description of the zoom objective lens design for 532 and 405 nm in detail.

Figure 10 shows a schematic diagram of the system. Structure of the recording disc is depicted in Fig. 10(a). The total thickness of the disc is 1.2 mm and recording material has a 0.6 mm of thickness. The recording material is formed on a $t = 0.6$ mm glass substrate, where a tracking groove is engraved by etching of the glass substrate.

The objective lens (object optics) focuses green light at the wavelength of 532 nm inside the recording material while it focuses red light (658 nm) on the groove of the glass substrate simultaneously. The second objective lens (reference optics) focuses green light (532 nm) and the two focused spots are formed. The two focused spots overlap on top of each other. As a result, a micrometer size Bragg grating is formed by the two counters propagating and mutually coherent beams.

For the 532 nm laser beam, the focusing depth measured from the surface of the disc is 0.7 – 1.1 mm. The focusing depth of the 658 nm laser beam is 0.6 mm. Due to the differences in the green and red focusing depth requires special consideration for the object optics in optical design.

Figure 10(b) shows the overall system layout. A 532 nm laser beam for writing and readout holograms is expanded and collimated. A 658 nm laser beam for tracking is expanded and collimated too. The green and red beams are combined by the dichroic mirror and are focused by the object optics. In the red optical path, a reflection from the

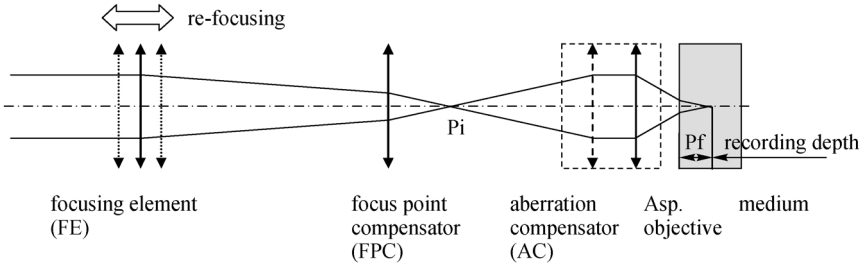

Fig. 8 Power arrangement of the variable focusing depth system having a constant focal length

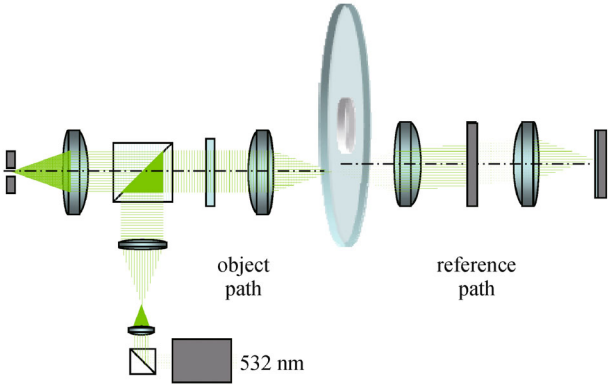

Fig. 9 Schematic diagram of multi-layer micro holographic data storage

groove is detected by a quad detector (QD). The signal from the QD is fed back to the lens actuator (now shown) to focus the red beam on the groove as well as track the groove. The focusing and tracking by the red beam is crucial to precisely overlap counter propagating green beams. For the purpose, a second QD is placed in the green optical path. When the objective lens in the object path is actuated by the servo system in 658 nm wavelength, the objective lens of the reference path is shifted along radial and tangential directions by observing the displacement and astigmatism at the QD in the green path. A Galvo mirror in the reference path shifts the lens in tangential direction. A standard voice coil actuator is used to shift the lens in radial direction and for focusing. The data is encoded in a streaming of a binary data. An electro optics modulator (EOM) modulates the laser beam record the binary bit stream as a sequence of hologram bits.

For readout, reference laser beam is blocked. The recorded micro hologram reflects the focused object beam and the reflected signal is detected by the QD in the green optical path.

As system overview describes, there are several important functionalities and constraints on optical designs to realize the system, including: 1) The recording depth varies, i.e., the aberrations within the range of recording depth (order of half millimeters) should be sufficiently small (< 0.1 waves in root mean square) for a NA of 0.4; 2) Two wavelengths of 532 nm for writing and reading out of the micro holograms and 658 nm for tracking and focusing are required. Also, lens aberrations need to be sufficiently small (< 0.1 waves in root mean square) for red wavelength; 3) All the optical components are off-the-shelf ones; And 4) off-the-shelf mechanical components are desirable too.

4 Design results and discussion

Figure 11 depicts the ray path of the core part of the system for 532 nm read and writes system. The optical components used for the design are commercially available off-the-shelf components. In the object path, there are four components (LP350080, LB1014, KBX037 and PAC034) are used. In the reference path, four components (LP352230, LB1258, KBX037 and PAC028) are used. The four components in each optical path correspond to aspheric OE, ACE, FPC and FE as depicted in Fig. 8. As described above, the OE, ACE and FPC are arranged so

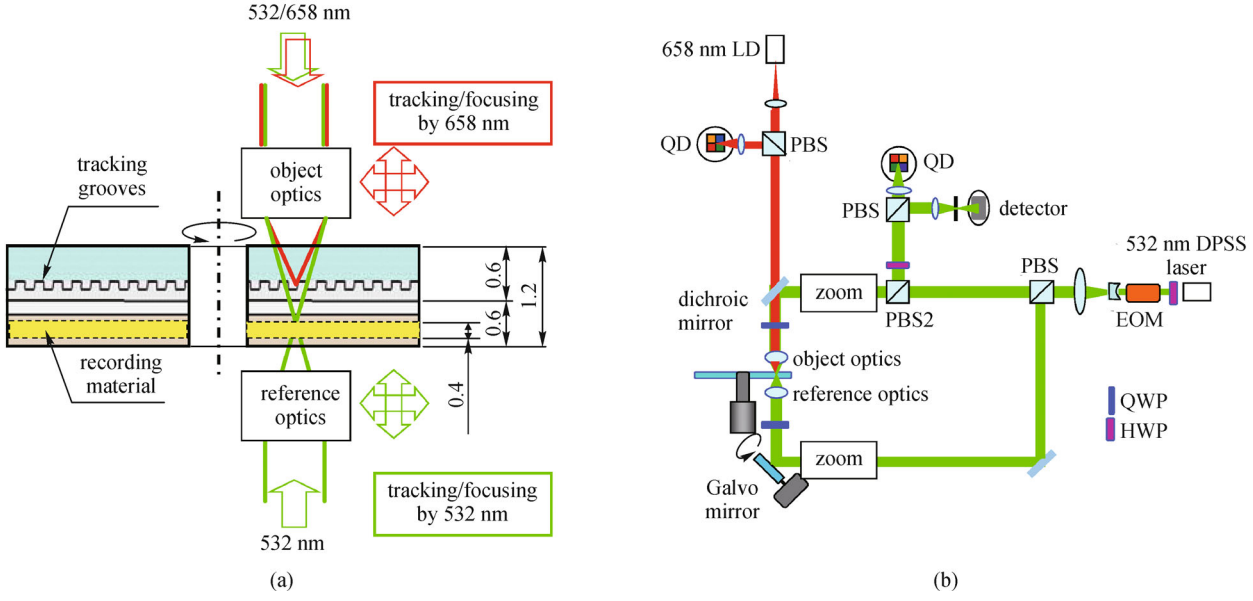

Fig. 10 Schematic diagram of multi-layer holographic recording demonstration platform. (a) Disc structure; (b) recording system. LD: laser diode; QD: quad detector; PBS: polarization beam splitter; EOM: electro optics modulator; DPSS: diode pumped solid state laser; QWP: quarter wave plate; HWP: half wave plate

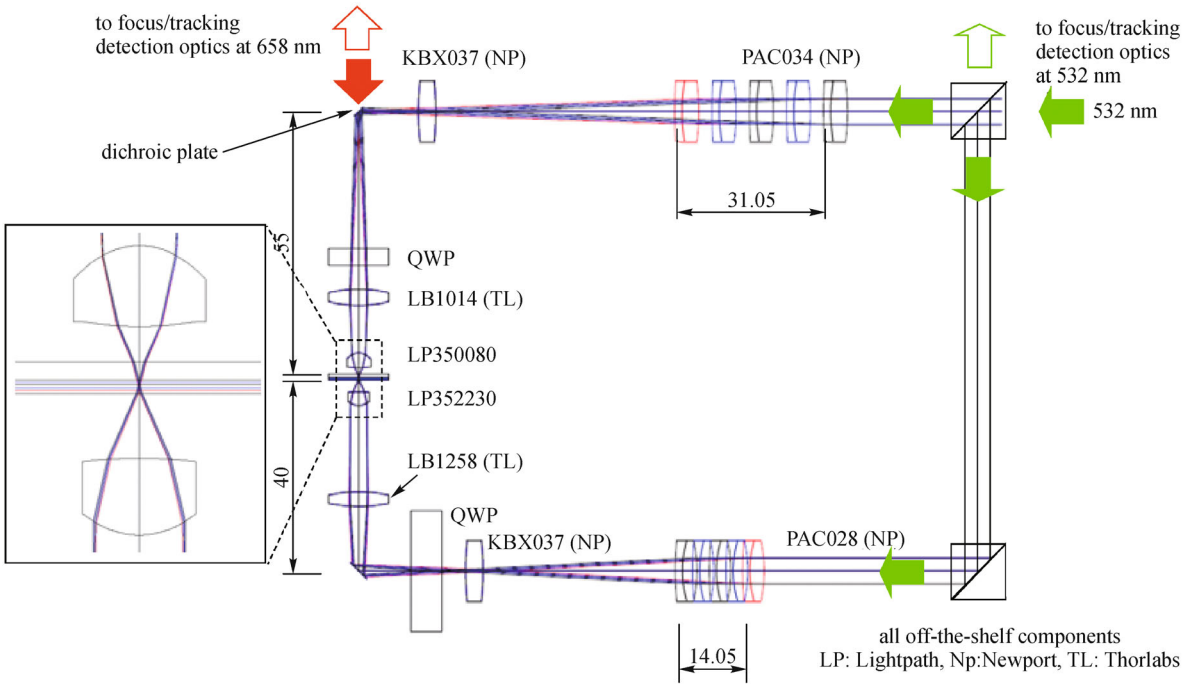

list of optical components

lens	supplier	diameter/mm	focal length/mm
PAC034	Newport	12.7	76.2
KBX037.AR14	Newport	12.7	62.9
LB1014.A	Thorlabs	12.7	25
LP350080	Lightpath Tech.	6.35	3.89
LP352230-A	Lightpath Tech.	6.35	4.51
LB1258.A	Thorlabs	12.7	30
PAC028	Newport	12.7	50.8

Fig. 11 Design results, writing and readout optics for 532 nm wavelength

that they work as an afocal system, or the combined focal length of the three elements is infinity. Since the depth of the recording layer extends from 0.7 to 1.1 mm from the surface of the disc, the object and reference optics are not identical. Optical design is performed as follows. At first commercially available aspheric objective lens is selected. Then other spherical components are incorporated with it. Without changing the lens data of the aspheric objective lens, other lens parameters are optimized while satisfying the proposed power arrangement. Then, the optimized system is fitted with the commercially available components that parameters are close to the optimized result. The process is repeated for a list of the commercially available aspheric lenses. Finally, the optimum design is identified by comparing system with different kinds of aspheric lenses used as a starting point. Since the object optics shares two wavelengths 532 and 658 nm for tracking and focusing servo, the object optics are optimized for both of the wavelengths. Optical design for 658 nm is shown in Fig. 12.

Table 2 shows paraxial data as a function of the recording depth for 532 nm object path depicted in Fig. 11. For each recording depth, effective focal length (EFL), back focal length (BFL), front focal length (FFL), NA, and wave aberration in root mean square are evaluated. The effective focal length varies from 0.3% to 1% with respect to nominal focal length values for object path. The variation of the back focal length is less than 1 μm. The back focal length is measured from the recording layer where the aberration is minimized. Therefore, the system is optimized while satisfying the paraxial requirements discussed in Section 3. The front focal length varies linearly with recording depth. Since the effective focal length is constant over the recording depth, therefore, the variation in the front focal length is solely attributed to the movement of the focusing element. The linearity between

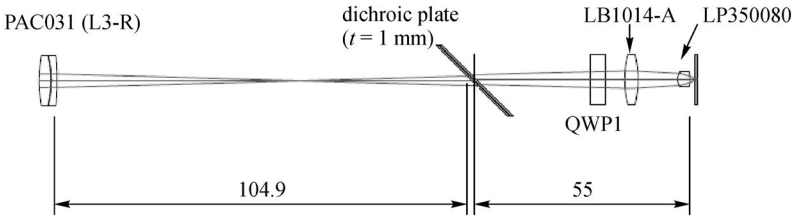

list of optical components

lens	supplier	diameter/mm	focal length/mm
LB1014.A	Thorlabs	12.7	25
LP350080	Lightpath	6.35	3.89
PAC031	Newport	12.7	63.5

Fig. 12 Design results, tracking and focusing optics for 658 nm wavelength

front focal length and recording depth assures linearity in zooming in the design. The NA is constant over the recording depth. Thus, Table 2 shows the key aspects of the design, suppressing variation of focal length over the range of recording depth and linearity in zooming. Wavefront error in root mean square is smaller than 0.017 waves over the recording depth.

Table 3 shows paraxial data as a function of the recording depth for 532 nm reference path depicted in Fig. 11. The focal length variation is smaller than 1% and is matched to the focal length of the object path optics. As a result, individual tuning of tracking and focusing servo gains in 532 nm are not required. The matched focal length simplifies the servo system design and enables precise overlapping of focused and counter propagating green beams. The variation in focal length and linearity of the movement of focusing element over the recording depth are assured to the reference path optics too with a similar range of focal length and linearity errors. Wavefront error in root mean square is smaller than 0.05 waves over the recording depth.

Table 4 shows paraxial data as a function of the recording depth for 658 nm path depicted in Fig. 11. The 658 nm path shares major optics with the 532 nm object path. The key aspect in the design is to achieve small wavefront error for 658 nm while not affecting the zooming and wavefront error performance for 532 nm. A similar design approach for the 532 nm optical system is used to select the most appropriate off-the-shelf components for the focusing element. Matching of the focal length to 532 nm focal length is not required since 658 nm servo system works as a master servo to control 532 nm servo systems of object and reference path. Wavefront error in root mean square is smaller than 0.017 waves at 0.6 mm recording depth, where tracking and servo grooves exist.

Figure 13 depicts tolerance analysis result. Wavefront error in root mean square is estimated by assuming standard lens tolerances of off-the-shelf components. In the analysis, the range of tracking and focusing is assumed as 0.2 mm. Under the condition, wavefront error as designed and as built is less than 0.1 waves for over all the recording depths.

Table 5 summarizes specifications and design results. The system is implemented by Shi et al. and successfully demonstrated writing and read out of micro holograms [16].

The design procedure for the 532 nm wavelength is also applicable for the 405 nm wavelength with minor modifications. All the lens elements used for the 405 nm system are identical to those of the 532 nm system, except for the optical components which have wavelength dependent performances, such as, 1) dichroic beam splitter to combine read/write beam (405 nm) with focusing and tracking beam (658 nm), 2) half and quarter wave plate used for the wavelength of 405 nm, and 3) polarized beam splitter usable for the wavelength of 405 nm. In addition, refocusing by moving the focusing element is needed due

Table 2 Paraxial data of the object path system for 532 nm

recording depth/mm	EFL (effective focal length)	BFL (back focal length)	FFL (front focal length)	NA (numerical aperture)	wave aberration (waves)
0.7	6.811	0.0005	−43.7489	0.4	0.0048
0.8	6.8157	0.0012	−36.0226	0.4	0.0077
0.9	6.8204	0.0016	−28.2747	0.4	0.0134
1.0	6.8252	0.0018	−20.5027	0.4	0.0166
1.1	6.8299	0.0016	−12.7032	0.4	0.0166

Table 3 Paraxial data of the reference path system for 532 nm

recording depth/mm	EFL (effective focal length)	BFL (back focal length)	FFL (front focal length)	FNO (F number)	wave aberration (waves)
0.7	6.8298	0.0002	−33.3701	0.4	0.0061
0.8	6.8476	0.002	−36.9458	0.4	0.0223
0.9	6.8652	0.0033	−40.4747	0.4	0.0332
1.0	6.8828	0.0041	−43.9589	0.4	0.039
1.1	6.9002	0.0044	−47.4002	0.4	0.0403

Table 4 Paraxial data of the tracking servo system for 658 nm

recording depth/mm	0.6
EFL (effective focal length)	3.8524
BFL (back focal length)	0.0001
FFL (front focal length)	68.8095
NA (numerical aperture)	0.45
wave aberration (waves)	0.0165

to the disc configuration (0.6 mm substrate/0.2 mm recording material/0.6 mm substrate). Also, to use a short coherence length 405 nm leaser, the optical path length difference of each arm is adjusted by adding a delay-line. Figure 14 depicts an optical design for 405 nm wavelength. Table 6 summarizes design objectives and design results. For the 405 nm system design, linearity in zooming and wavefront error is comparable to those for 532 nm design. Note that the range of the recording depth is 0.2 mm compared to 0.6 mm for the 532 nm design. The smaller focusing range is due to the disc structure but not limited by the optical design.

5 Conclusions

In designing optical systems for volumetric optical recordings, physical mechanism to achieve a high recording density determines fundamental optical design specifications. Bragg selectivity in volume holographic recording requires Anastigmatic lens designs to perform a well-defined mapping of data pixel locations to angular spectrum components in Fourier domain. For volume holographic recording optics, 1st order and 3rd order optical design study reveals that at least five aberrations have to be corrected among the nine object and pupil Seidel aberrations.

For multi-layer volumetric recording, it is essential to have aplanatic designs with zooming capabilities to access to multiple recording layers. In addition, it is needed to have a constant focal length, linearity between moving element to the recording depth, and spherical aberration correction induced by the variable recording depth.

Aplanatic objective lens with single moving element can be usable as far as conjugate ratio for the objective lens is not substantially altered while zooming. However, it is desirable to implement an afocal sub part in the optical train. The afocal part, consist of high NA objective lens and additional compensating lenses, takes crucial role for the optics in multi-layer volumetric recording. By the afocal sub part, it becomes feasible to satisfy multiple requirements for optics, such as a constant focal length, linearity between moving element to the recording depth. The zoom design with an afocal part can be minimally designed as a three-element system that consists of a zooming element, a compensator, and a high NA objective lens. Design study shows that it is needed to add one additional element between the compensator and the high NA objective lens. For an objective lens designed for infinite conjugate ratio, four element design is preferable

Table 5 Summary of design specifications and results

			specifications	results
1	disc type		$t = 0.6\,\text{mm} + 0.6\,\text{mm}$	←
2	wavelength/nm	recording	532	←
3		focusing/tracking	658	←
	NA (numerical aperture)	recording	0.4	0.4
		focusing/tracking	0.45	0.45
4	recording depth/mm		0.7–1.1 (range of the depth: 0.4)	0.7–1.1
5	focusing/tracking depth/mm		0.6	0.6
6	wavefront error	532 nm	0.1 waves in RMS as built, object height < 0.03 mm	0.1
		658 nm	0.1 waves in RMS as built, object height < 0.03 mm	0.1
7	other requirements		off-the-shelf lenses	←

Note: RMS: root mean square

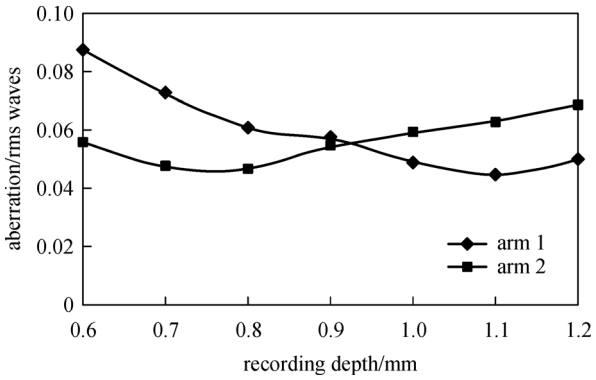

Fig. 13 Result of tolerance analysis. As built performance as a function of recording depth for objective (arm 1) and reference (arm 2) optical path

Table 6 Design specifications and design results for 405 nm wavelength

			specifications	results
1	disc type	blue sensitive	t = 0.6 mm disc/t = 0.2 mm recordable disc/t = 0.6 mm disc	←
2	wavelength/nm	recording	405	←
		focusing/tracking	658	←
3	NA (numerical aperture)	recording	0.4	←
		focusing/tracking	0.45	←
4	recording depth/mm)		0.6 – 0.8 (range of the depth: 0.2)	←
	(405 nm)			
5	focusing/tracking depth/mm		0.6 mm	←
	(658 nm)			
6	wavefront error	405 nm	0.1 waves in RMS, object height < 0.03 mm	←
		658 nm	0.1 waves in RMS, object height < 0.03 mm	←
7	other requirements		off-the-shelf lenses	←

Note: RMS: root mean square

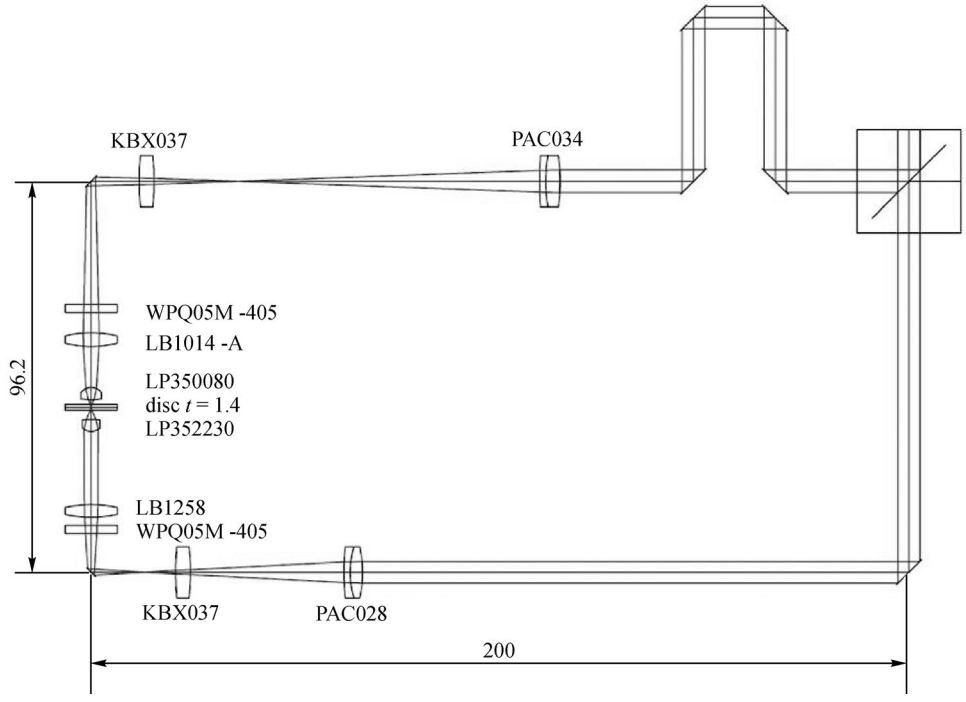

Fig. 14 Design results, writing and readout optics for 405 nm wavelength

since the design keeps the angle of incidence of marginal rays close to the angle for which the objective lens is designed. In addition, the four element design suppresses variation of spherical aberration during zooming. Based on the four element configuration, an NA 0.4 system has been designed with a recording depth range of 0.4 mm. Such a design is feasible by using four elements for the core part of the design along with commercially available objective lens designed for non-zooming purposes. In addition, tracking and focusing capabilities are implemented by using only off-the-shelf components. For the design, as built wavefront error over the recording depth range is estimated as small as 0.1 waves in root mean square for 532 nm wavelength. The design allows the use of 405 nm with minor modifications.

Acknowledgements The initial design works for the multi-layer holographic data storage was carried out at Stanford University under the support from GE Global Research Center. The support was gratefully acknowledged.

References

1. Ashton K. That ‘internet of things’ thing: in the real world things matter more than ideas. RFID Journal, 2009, 22: 97–114
2. McLeod R R, Daiber A J, McDonald M E, Robertson T L, Slagle T, Sochava S L, Hesselink L. Microholographic multilayer optical disk data storage. Applied Optics, 2005, 44(16): 3197–3207
3. Takashima Y, Hesselink L. Design and tolerance of numerical aperture 0.8 objective lenses for page-based holographic data storage systems. Japanese Journal of Applied Physics, 2009, 48 (3S1): 03A004
4. Neifeld M A, McDonald M. Lens-design issues affecting parallel readout of optical disks. Applied Optics, 1995, 34(23): 5167–5174
5. Neifeld M A, McDonald M. Lens design issues impacting page access to volume optical media. Optics Communications, 1995, 120 (1–2): 8–14
6. Zeng J Y, Wang M Q, Yan Y B, He Q S, Jin G F. Design of a short-focal-length double-Fourier-transform-lens system for holographic storage. Optical Engineering (Redondo Beach, Calif.), 2007, 46(3): 033002-1–033002-7
7. Kubota S. Aplanatic condition required to reproduce jitter-free signals in an optical digital disk system. Applied Optics, 1987, 26 (18): 3961–3973
8. Stallinga S. Compact description of substrate-related aberrations in high numerical-aperture optical disk readout. Applied Optics, 2005, 44(6): 849–858
9. Barbastathis G, Psaltis D. Volume Holographic Multiplexing Methods. In: Coufal H J, Psaltis D, Sincerbox G T, eds. Holographic Data Storage. Springer Berlin Heidelberg: Springer, 2000, 21–62
10. von Bieren K. Lens design for optical fourier transform systems. Applied Optics, 1971, 10(12): 2739–2742
11. Orlov S S, Phillips W, Bjornson E, Takashima Y, Sundaram P, Hesselink L, Okas R, Kwan D, Snyder R. High-transfer-rate high-capacity holographic disk data-storage system. Applied Optics, 2004, 43(25): 4902–4914
12. Wynne C G. Primary aberrations and conjugate change. Proceedings of the Physical Society, 1952, 65(6): 429–437
13. Matsui Y, Nariai K. Fundamentals of Practical Aberration Theory: Fundamental Knowledge and Techniques for Optical Designers. New Jersey: World Scientific, 1993
14. Milster T D, Upton R S, Luo H. Objective lens design for multiple-layer optical data storage. Optical Engineering (Redondo Beach, Calif.), 1999, 38(2): 295–301
15. Eichler H J, Kuemmel P, Orlic S, Wappelt A. High-density disk storage by multiplexed microholograms. IEEE Journal on Selected Topics in Quantum Electronics, 1998, 4(5): 840–848
16. Shi X, Ostroverkhov V, Lawrence B, Boden E, Ren Z, Takashima Y, Ross F. Micro-holographic data storage: materials and systems. Review of Laser Engineering, 2010, 38: 349–355

Yuzuru Takashima is an Associate Professor at College of Optical Sciences of University of Arizona and has been on the faculty since 2011. He teaches one of the core courses: Lens Design for undergraduates and Optical Design for Multi-scale Photonic System for graduate students. Prior to joining to the University of Arizona, he was employed as a research staff by Stanford University, where he has been actively involved in the field of novel optical system design and engineering, particularly for high density page-based and bit-based holographic data storage systems and Nano-photonic electron beam generators. He was employed as an optical engineer at Toshiba Corporation in Japan, where he conducted research and development of ultra-precision manufacturing of optical components and products. He received his B.S. degree in Physics from Kyoto University (1990) and M.S. (2004) and Ph.D. degrees in Electrical Engineering from Stanford University in 2007. His current research includes X-ray optical system design, environmentally robust holographic data storage system, mask-based and mask-less hybrid lithography for 3D optical interconnects, novel alignment process for lithography, ultra-thin form factor head worn display, and environmentally robust free space quantum optical communication system.